

ESD RELATED R&D STUDIES AT CNES AND ONERA

Denis PAYAN⁽¹⁾, Virginie INGUIMBERT⁽²⁾, Jean-Charles MATEO-VELEZ⁽²⁾,
 Daniel SARRAIL⁽²⁾, Thierry PAULMIER⁽²⁾, Jean-François ROUSSEL⁽²⁾,
 Bernard DIRASSEN⁽²⁾, Françoise BOULAY⁽²⁾, Laurence GIRARD⁽³⁾

⁽¹⁾ CNES
 18 Avenue Edouard Belin
 31 401 Toulouse cedex 9
 France

⁽²⁾ ONERA DESP
 2 Avenue Edouard Belin
 31055 Toulouse cedex 4
 France

⁽³⁾ CRIL ALYOTECH
 6 rue Brindejonc les moulinais
 31500 Toulouse
 France

1 - INTRODUCTION

The paper presents the experimental and numerical capabilities of CNES and ONERA Space Environment Department on charging and Electrostatic discharges (ESD) studies. In a first part, the SIRENE spectrum is presented; dose and temperature effects on material conductivity are studied. In the second part, the Inverted Voltage Gradient situation is obtained on a large solar array in the plasma chamber JONAS and the flash over is measured. Finally, the last numerical simulations (plasma chamber and ESD inception) performed with SPIS are presented.

2 - DEEP DIELECTRICS CHARGING

2.1 - GEOSTATIONARY ORBIT ELECTRON FLUX - REFERENCE SPECTRUM

The utilization in the SIRENE facility of a realistic spectrum sets the problem of choosing the best worst case energy spectrum of the GEO like environment. Tests has to be representative for all the experimental simulation of the electrostatic charging and discharging phenomena made in laboratory. The CNES and ONERA DESP has adopted the spectrum SIRENE presented in Figure 1.

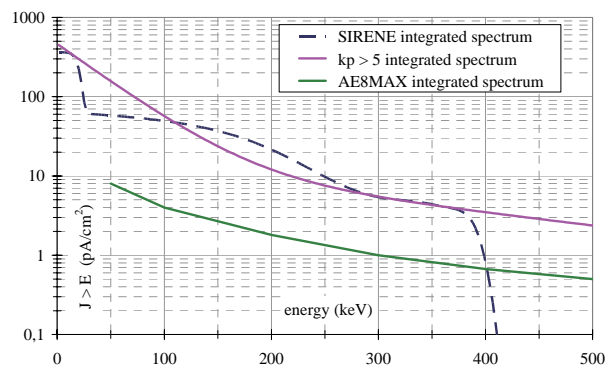


Figure 1 – SIRENE spectrum

2.2 - SIRENE EXPERIMENTAL FACILITY

The originality of the SIRENE experimental simulation facility is that it includes equipment making it possible to reproduce the effects of the charges induced by the electrons from the space

environment in an energy range lower than or equal to 400 keV. The SIRENE facility has the following main components:

- A large-dimension cylindrical vacuum chamber ($L \approx 1.5$ m, $\varnothing \approx 0.5$ m) designed in 3 sections to ensure modularity. The horizontal opening of the chamber makes it easy to set up experiments *in situ*. At the level of the vessel, the influence of the terrestrial magnetic field on the electron flow trajectory is compensated for by the magnetic field induced by the two pairs of windings (vertical and horizontal) surrounding the chamber. The body of the chamber is fitted with several standardised diameter extensions enabling the installation of various control and metrology instruments (vacuum gauge, visualisation camera, electrical outputs, analysis probes, connections to the radiation sources, etc.).
- A primary and secondary pumping unit which ensures a pressure of the order of 10^{-6} hPa after some hours in operation.
- A specimen door, with temperature regulation within a range comprised between -180°C and $+100^{\circ}\text{C}$.
- The facility is equipped with two electron sources:
 - a Van de Graaff type accelerator capable of delivering a monoenergetic electron beam whose energy level can be adjusted between 100 and 400 keV. In the case of experiments carried out using a simulation of electron flux from space whose energy spectrum is distributed, the accelerator's operating energy is of the order of 400 keV (most frequent case).
 - a low-energy electron gun which delivers a beam whose energy level can be adjusted between 1 and 35 keV. This electron beam can be used alone (many tests are requested on the basis of specifications such as: $E=20$ keV, $\Phi=1$ nA/cm²). It is also used to complete the flow of the Van de Graaff accelerator's electron beam at low energy levels.
- A set of "complex" diffusion windows designed to transform the 400 keV monoenergetic beam delivered by the accelerator into an energy-distributed beam according to a reference spectrum chosen to simulate a type of orbit.
- The analysis instruments specific to the electrostatic studies, that is to say:
 - current probes for detecting discharges and analysing current transients,
 - a potential probe used for analysing charge potentials along a vertical axis.

A further development phase being carried out at present with the CNES concerns the metrology of the charge potentials. The instruments currently in place only enable *in situ* measurements of the potentials according to a vertical axis ($d \leq 15$ cm) and no other analysis probe movements are possible. In the case of studies on a relatively large number of simple specimens, or on more complex structures (solar arrays, antennas, etc.), these instruments are insufficient. Consequently, a new potential probe movement system is in the process of being designed. It should make it possible to analyse charge potentials in a 20 cm x 20 cm plane.

A general view of the SIRENE experimental facility is shown in Figure 2.

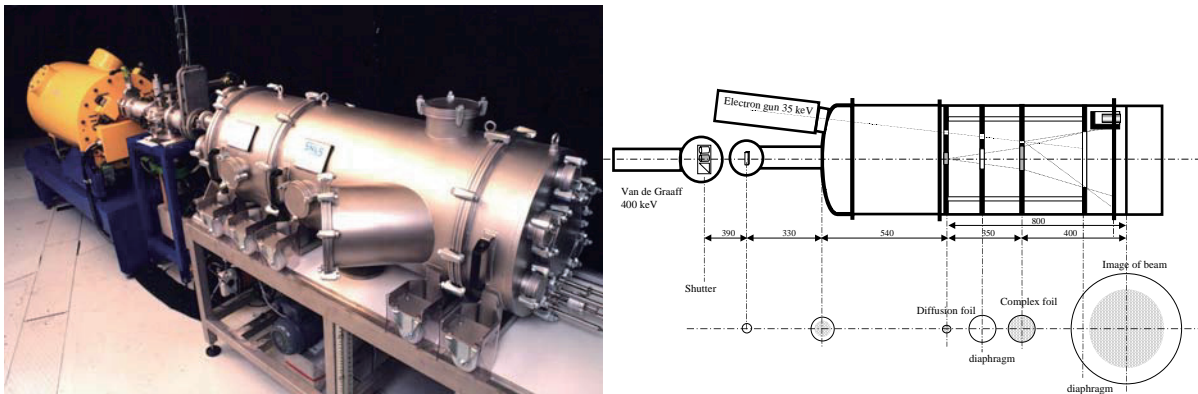


Figure 2: General view & schematic diagram of SIRENE

The facility's various components with the positioning and the trajectory of the two electron beams delivered by the electron gun and the Van de Graaff accelerator are symbolised in Figure 2 (shown in the horizontal plane). The SIRENE integrated spectrum (GEO orbit) is compared with the $Kp > 5$ integrated reference spectrum in Figure 1, and a good match can be seen between the two spectrums.

2.3 - TEMPERATURE EFFECT

The influence of the temperature on deep dielectrics charging is studied using the SIRENE integrated spectrum. The effect is weak in the case of a 50 μm thick layer of Kapton® because this material has a good Radiated Induced Conductivity (RIC). On the contrary, the effect is strong on a solar cell like device, composed of glued CMX. The conductivity is highly decreased for temperatures less than 0°C, Figure 3.

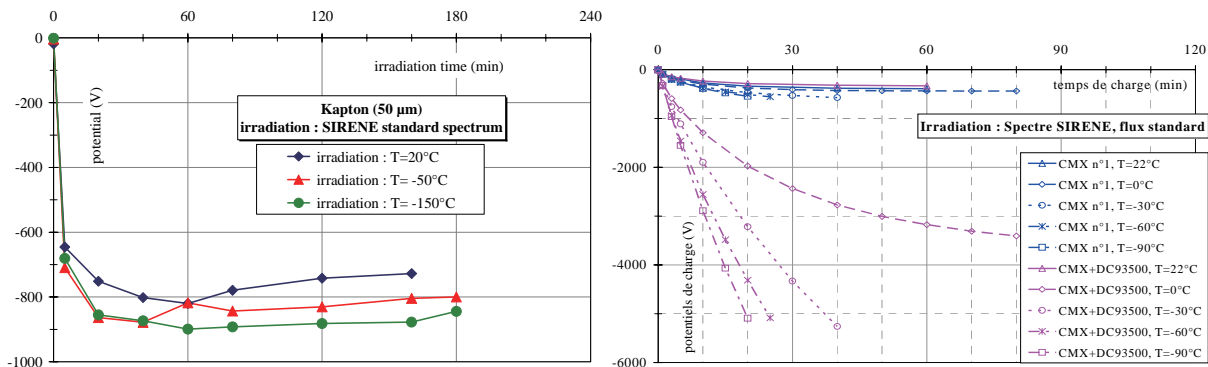


Figure 3 – Temperature effect on Kapton conductivity (left) and on CMX and glued CMX (right)

3 - FLASH-OVER ON SOLAR ARRAY COUPONS

3.1 - JONAS PLASMA CHAMBER

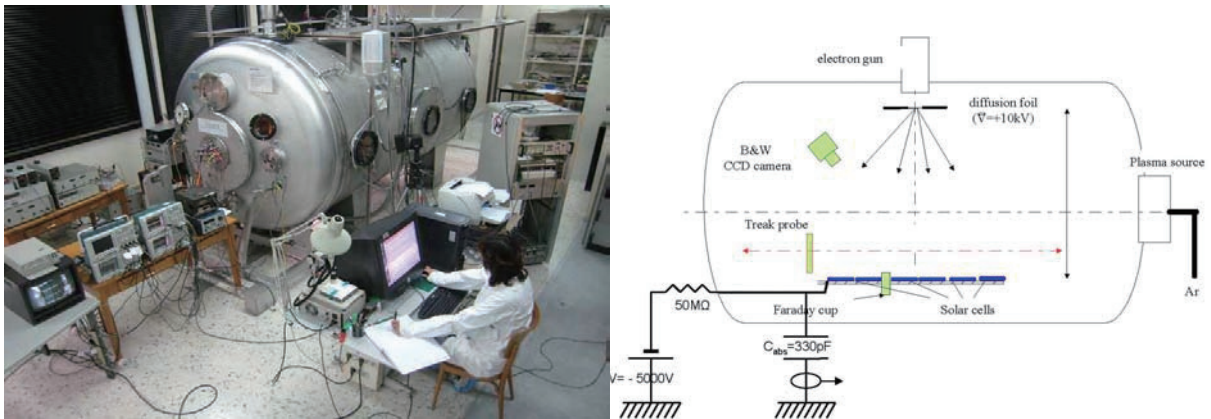


Figure 4 – JONAS Plasma chamber (left); solar panel test (right)

This set-up is a large chamber (L=3.5 m, $\varnothing=1,85$ m) built in a nonmagnetic stainless steel. A set of Helmholtz coils can compensate the earth magnetic field. A high capacity cryogenic pumping system (12000 l/s for argon gas) insures a limit pressure of 2.10^{-8} hPa after about fifteen hours of pumping. The set-up allows us to reproduce the Inverted Potential Gradient (IPG) situation observed in flight, i.e. while the satellite body (here sample structure and cells) is negatively charged up to several kilovolts, the dielectrics (here cover-glasses protecting the cells) build up a differential charge as high as 1000V. This can be reproduced either with plasma or electrons (ref). For this purpose, both plasma source and electron gun are implanted in the chamber. The plasma source is implanted in chamber axis (at one end) and allows us to reproduce low earth orbit plasma conditions with regards with electrostatic problems. On the other end of the chamber, the door is equipped with high voltage

and high current feedthroughs and receives the sample holder. On the top of the chamber are placed the electron gun and its diffusion foil. A photograph of JONAS chamber with all instruments required for ESD tests on solar arrays coupons and the schematics are presented in Figure 4. It shows a side view of the chamber with the implantation of all the different instruments.

3.2 - MAIN RESULTS

A large amount of tests have been performed on different size samples (from 2 X 3 cells to 19 X 16 cells coupons). The main results shows that:

- the flash-over can neutralize more than 1 m²,
- it extends more than 1.4 m with a velocity of about 10⁴ m/s,
- the flash-over can jump from a solar panel to another, even if these two panels have a 0.2 m gap distance.
- the secondary arcs durations is strongly dependant on coupon size (i.e. flash-over duration) : for the same couple (V, I) applied in the active gap, large coupon produces longer discharges than small one. Complementary tests have been performed using external capacitor as missing coverglasses simulator. The conclusion of this campaign is that this device is not realistic because using high values of external capacitance induces the creation of anodic spots on nearby ground leading to high plasma density increasing strongly the plasma conductivity and the available current in the ESD which becomes a Coupling with ground ESD (CwG ESD) as reported in our papers in 10th SCTC.

4 - SPIS LAST SIMULATIONS

4.1 - GLOBAL SIMULATION OF JONAS

The Spacecraft Plasma Interaction Software (SPIS) has been used to numerically simulate the physics in the plasma tank JONAS. The goal is to simulate both fast and slow ions co-existing in such ground plasma chamber. The plasma source is derived from the experimental results (density measurements with Langmuir probes upstream and downstream a plate). These fast ions are computed through a Monte-Carlo method. The neutrals are injected in the whole plasma tank volume. Their density is estimated by the measured residual pressure P_n .

The plasma dynamics consists in a PIC (Particle-In-Cell, Monte-Carlo) method for fast and slow ions. The electrons follow a Boltzmann distribution:

$$N_e = N_0 \exp\left(\frac{e\phi}{k_B T_e}\right)$$

where N_0 is a numerical parameter for the cutting of the Boltzmann distribution. When the plasma potential is positive, the electron density is set equal to N_0 .

The neutral dynamics is not calculated (constant pressure). The only volumetric reaction considered is the charge exchange (CEX) between fast ions and neutrals : $Ar_f^+ + Ar \rightarrow Ar + Ar_s^+$. The variation of the slow ion density during the time step dt is proportional to the neutral and fast ion densities $N(Ar_f^+)$ and $N(Ar)$:

$$\Delta N(Ar_s^+) = N(Ar_f^+) \cdot N(Ar) \cdot \sigma \cdot V_{rel} \cdot dt$$

where σ is the cross section of CEX reaction and V_{rel} the relative velocity of neutrals and fast ions. Fast ion and neutral densities are assumed to be conserved. Indeed, for $\sigma=10^{-18}m^2$ and $N(Ar) = 10^{17}m^{-3}$, the CEX ions reach 10% of the fast ions over a distance of 1m. The reaction rate is too small to have a strong effect on fast ions.

The electric field follows the non-linear Poisson equation:

$$-\Delta\phi = \frac{e}{\epsilon_0} \left(N_+ - N_0 \exp\left(\frac{e\phi}{k_B T_e}\right) \right)$$

The numerical parameters used in this study are presented on the following table. The fit of the fast ion beam measurement is used as an input data. The SPIS model is an axisymmetric source.

Simulation time (s)	Max integration time step (s)	N_0 (m ⁻³)
$2.5 \cdot 10^{-3}$	10^{-4}	10^{14}
σ (m ²)	Fast ion current (mA)	P_n (mbar)
$0.4 \cdot 10^{-18}$	1,1	$4.3 \cdot 10^{-6}$
Electron temperature (eV)	Tank voltage (V)	
0,2	-2	

4.2 - NUMERICAL RESULTS

The space distributions of fast and slow ion densities are presented in Figure 5. They are represented in the same logarithmic scale range so as to compare them.

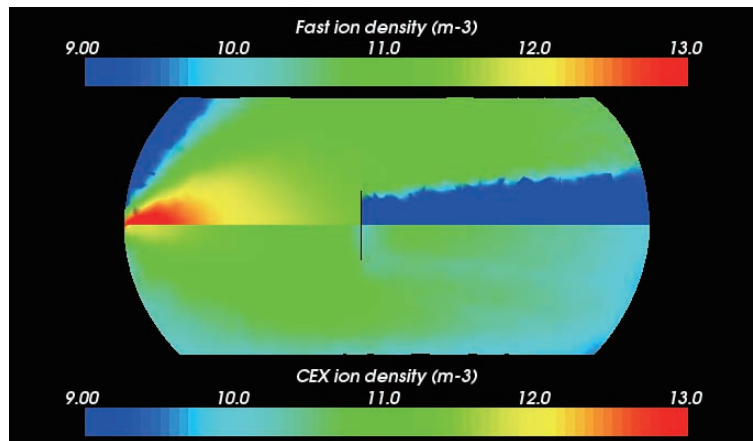


Figure 5- Fast (up) and slow (down) ion densities (logarithm scale)

The fast ion beam clearly shows a spatial decay corresponding to the divergence of the plasma plume. The fast ion density decreases from 10^{14} m^{-3} to 10^{11} m^{-3} at the back of the plasma tank. The aperture angle of 80° is well represented and the wake effect due to the plate is clearly demonstrated. The slow ions reach the whole tank due to their slow temperature. They are created in the vicinity of the plasma source and are submitted to potential gradients created by the fast ions. That makes them drift slowly towards the whole tank. Their density is about $10^{10} - 10^{11} \text{ m}^{-3}$.

4.3 - ESD TRIGGERING MODEL

SPIS has been used to simulate the first step of the ESD on the IVG obtained on solar cells. The geometrical model takes into account the triple point existing between the cell, the coverglass and the vacuum. This situation is enhanced by a micro tip, Figure 6.

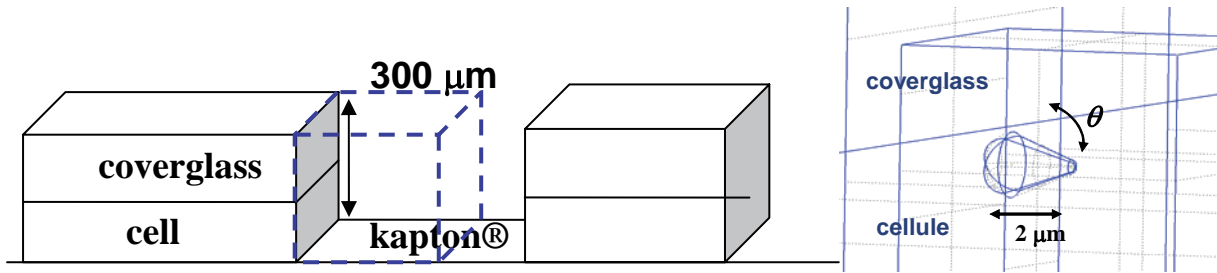


Figure 6 – Numerical model for the triple point geometry on solar cell

Electron dynamics is influenced by photoemission, secondary emission yield more than one in the coverglass and field effect on the cathode tip. The results, cf. Figure 7, show that the electric field is highly enhanced if the tip is oriented towards the coverglass. This situation amplifies the field effect electron emission. These so created electrons collide with the dielectrics and produce secondary emission. The positive charge induced then increases the electric field and so on, up to the beginning of the ESD.

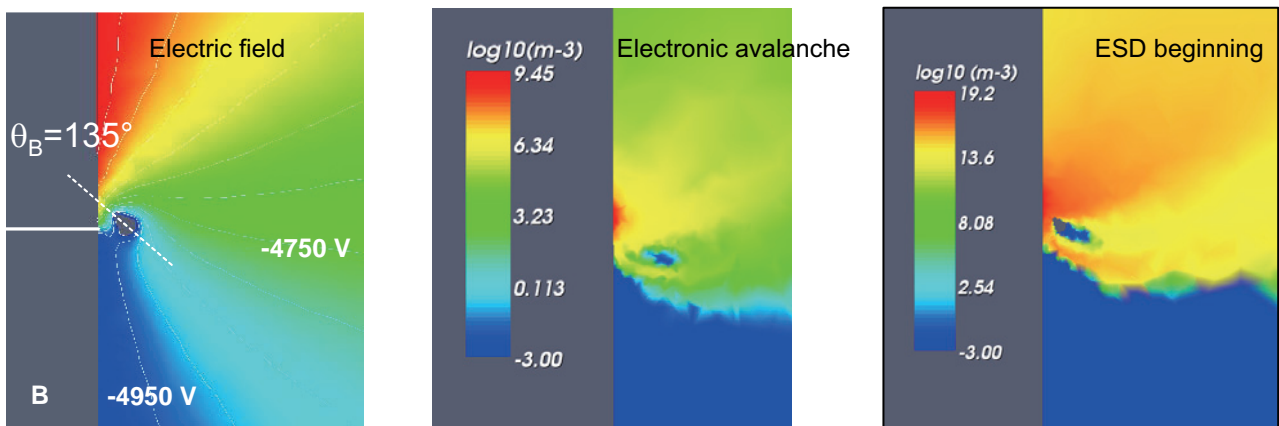


Figure 7 – Electric field amplification (left), electronic avalanche (middle) and ESD inception (right) in the IVG model

5 - CONCLUSION

For each study at CNES and ONERA, we follow a global approach consisting in:

- understanding and modelling the physics,
- developing flight representative facilities (SIRENE, JONAS, ...) and associated setups,
- performing flight representative experiments,

because all R&D studies depend strongly on test setup configurations especially ESD qualification of materials and assemblies.

6 - REFERENCES

- [1] Effect of a realistic charging environment on electrostatic qualification for space dielectrics, Payan et al., 10th Spacecraft Charging Technology Conference, Biarritz, France, June 2007
- [2] Electrotatic discharge and secondary arcing on solar array - Flash-over measurement and consequences on arc occurrence - Dependence with the test set-up, Payan et al., 10th Spacecraft Charging Technology Conference, Biarritz, France, June 2007
- [3] Ground plasma tank modelling and comparison to measurements. J.C. Matéo-Vélez et al., 10th Spacecraft Charging Technology Conference, Biarritz, France, June 2007

- [4]** Simulation of an electrostatic discharge initiation with software SPIS, L. Girard et al., 10th Spacecraft Charging Technology Conference, Biarritz, France, June 2007